

## Effect of N/Ga flux ratio on transport behavior of Pt/GaN Schottky diodes

Basanta Roul, Mahesh Kumar, Mohana K. Rajpalke, Thirumaleshwara N. Bhat, Neeraj Sinha, A. T. Kalghatgi, and S. B. Krupanidhi

Citation: *J. Appl. Phys.* **110**, 064502 (2011); doi: 10.1063/1.3634116

View online: <http://dx.doi.org/10.1063/1.3634116>

View Table of Contents: <http://aip.scitation.org/toc/jap/110/6>

Published by the [American Institute of Physics](#)

---

---

## Effect of N/Ga flux ratio on transport behavior of Pt/GaN Schottky diodes

Basanta Roul,<sup>1,2</sup> Mahesh Kumar,<sup>1,2</sup> Mohana K. Rajpalke,<sup>1</sup> Thirumaleshwara N. Bhat,<sup>1</sup> Neeraj Sinha,<sup>3</sup> A. T. Kalghatgi,<sup>2</sup> and S. B. Krupanidhi<sup>1,a)</sup>

<sup>1</sup>Materials Research Centre, Indian Institute of Science, Bangalore-560012, India

<sup>2</sup>Central Research Laboratory, Bharat Electronics, Bangalore-560013, India

<sup>3</sup>Office of Principal Scientific Advisor, Government of India, New Delhi-110011, India

(Received 7 April 2011; accepted 4 August 2011; published online 16 September 2011)

GaN films were grown on c-plane sapphire by plasma-assisted molecular beam epitaxy (PAMBE). The effect of N/Ga flux ratio on structural, morphological, and optical properties was studied. The dislocation density found to increase with increasing the N/Ga ratio. The surface morphology of the films as seen by scanning electron microscopy shows pits on the surface and found that the pit density on the surface increases with N/Ga ratio. The room temperature photoluminescence study reveals the shift in band-edge emission toward the lower energy with increase in N/Ga ratio. This is believed to arise from the reduction in compressive stress in the films as is evidenced by room temperature Raman study. The transport studied on the Pt/GaN Schottky diodes showed a significant increase in leakage current with an increase in N/Ga ratio and was found to be caused by the increase in pit density as well as increase in dislocation density in the GaN films. © 2011 American Institute of Physics. [doi:10.1063/1.3634116]

### I. INTRODUCTION

In recent times, GaN-based materials have received considerable attention due to their potential applications in light-emitting diodes (LEDs), high electron mobility transistor (HEMTs), laser diodes, UV detectors, and high temperature/high power electronics.<sup>1-5</sup> The most attractive property of GaN is its direct wide bandgap ( $\sim 3.4$  eV),<sup>6</sup> which allows an efficient emission at room temperature. GaN can be alloyed with AlN and InN,<sup>7-9</sup> which allows tuning of the bandgap and emission wavelength ranging from ultraviolet (UV) to near infrared (IR) region. However, since the lattice parameter and thermal expansion coefficient of GaN are not well matched to the underlying sapphire substrate, the epitaxial growth of GaN generates huge densities of dislocations,<sup>10-12</sup> which largely affects the electronic and optical properties. However, there are some novel methods like epitaxial lateral overgrowth (ELO),<sup>13</sup> use of appropriate nucleation layers,<sup>14</sup> etc. that can reduce the density of dislocation in the films and may lead to improvements in the performance of GaN-based optoelectronic devices. The understanding of the growth condition of GaN films and its effect on metal contacts to GaN are also an important issue, because the performance of the GaN based devices can be limited by the quality of the films. In this work, we have grown GaN epitaxial films on c-sapphire by plasma assisted molecular beam epitaxy with different N/Ga flux ratio and studied the effect of flux ratio on structural and optical properties. The electrical characteristics of Schottky contacts to GaN have also been investigated. In regard to Schottky behavior study, we have fabricated Pt/GaN Schottky diodes and studied the effects of N/Ga flux ratio on electrical characteristics based on thermionic emission model.

### II. EXPERIMENTAL PROCEDURES

The GaN films used in this study were grown on a sapphire substrate by plasma-assisted molecular beam epitaxy. Prior to growth, the sapphire substrates were degreased with organic solvents, and etched in a hot solution of H<sub>2</sub>SO<sub>4</sub> and H<sub>3</sub>PO<sub>4</sub> (H<sub>2</sub>SO<sub>4</sub>: H<sub>3</sub>PO<sub>4</sub> = 3:1) for 20 min, rinsed with de-ionized water and then dried with nitrogen gas. The substrates were thermally cleaned at 750 °C for 30 min and then subjected to nitridation treatment for 30 min at 700 °C. After substrate nitridation, the films were grown by using two step processes, growth of low temperature GaN buffer layer of thickness 20 nm at 500 °C followed by high temperature (750 °C) epilayers. The samples investigated in this study were grown for 3 h with different N/Ga flux ratio. Here, we varied the nitrogen beam equivalent pressure (BEP), while the gallium BEP was kept  $5.6 \times 10^{-7}$  mbar to obtain the different N/Ga flux ratio. The N/Ga ratios for the samples were 18.8 (sample-A), 29.4 (sample-B), and 40.1 (sample-C). RF power of nitrogen plasma was kept constant at 350 W for all the growth. The as-grown samples were characterized by high-resolution x-ray diffraction (HRXRD), scanning electron microscopy (SEM), room temperature photoluminescence (PL) spectroscopy, and Raman spectroscopy. The structural characterization of GaN films were carried out by HRXRD measurements using a double crystal four-circle diffractometer (Bruker-D8 DISCOVER) with Cu K $\alpha$  ( $\lambda = 1.5418$  Å) radiation. The surface morphology of the grown samples was observed by SEM measurements using high resolution field emission FEI (SIRION) system. Room temperature PL was carried out by using He-Cd laser with 325 nm wavelength. Raman spectroscopy measurements were used for strain analysis of the films and were carried out using Ar<sup>+</sup> laser with 514 nm wavelength. The electrical characteristics of Schottky contact to GaN have investigated. For this, we fabricated Pt/GaN Schottky diodes and studied

<sup>a)</sup>Electronic mail: sbk@mrc.iisc.ernet.in.

the effects of N/Ga flux ratio on electrical transport properties. The inner circular Schottky contact of diameter  $600 \mu\text{m}$  was made on GaN films by depositing Pt (200 nm) metal using RF-sputtering. Then, the outer circular ohmic contact of diameter  $1000 \mu\text{m}$  was made by thermally depositing Al (thickness  $\sim 200 \text{ nm}$ ) metal. Finally, the device was annealed at  $200^\circ\text{C}$  for 20 min. The room temperature  $I$ - $V$  measurements were performed by taking one contact from Pt metal and another from Al metal by using computer interfaced Agilent-4155 source meter system. The room temperature Hall measurements were performed on the GaN samples to determine the nature of current transport mechanism present in the Schottky diodes.

### III. RESULTS AND DISCUSSION

Figure 1 shows a  $2\theta$ - $\omega$  HRXRD scan of GaN films grown on c-plane sapphire substrate. The peaks at  $2\theta = 34.56^\circ$  and  $72.81^\circ$  are assigned to the (0002) and (0004) planes of the GaN films. The strong peak at  $2\theta = 41.69^\circ$  is assigned to the  $\text{Al}_2\text{O}_3$  (0006) reflection. The structural quality of the films was evaluated from the X-ray  $\omega$ -scan rocking curves. In GaN films there are different kinds of threading dislocations (TDs) present, like screw TDs, edge TDs and mixed TDs, which affect the FWHM of X-ray rocking curves. The X-ray rocking curves for symmetric (002) and asymmetric (102), (104), (105), and (121) GaN reflections were carried out. The FWHM values for different reflections are given in Table I. It is found that the FWHM of the asymmetric reflection is higher than the FWHM of symmetric reflections, i.e., the GaN films are defective structure with a large edge TDs.<sup>15</sup> The rocking curve of the symmetric (002) and asymmetric (121) GaN reflections are shown in the Fig. 2. The dislocation density of the GaN films were estimated from the following equations:<sup>16</sup>

TABLE I. The FWHM (deg.) of both symmetric and asymmetric X-ray rocking curves.

Reflection	(a); N/Ga = 18.8	(b); N/Ga = 29.4	(c); N/Ga = 40.1
(002)	0.20	0.27	0.34
(102)	0.47	0.50	0.52
(104)	0.33	0.38	0.42
(105)	0.29	0.34	0.38
(121)	0.57	0.64	0.69

$$D_{\text{screw}} = \frac{\beta_{(002)}^2}{9b_{\text{screw}}^2}, \quad D_{\text{edge}} = \frac{\beta_{(121)}^2}{9b_{\text{edge}}^2}, \quad (1)$$

where  $D_{\text{screw}}$  is the screw dislocation density,  $D_{\text{edge}}$  is the edge dislocation density,  $\beta$  is the FWHM of the measured XRD rocking curves, and  $b$  is the Burgers vector length ( $b_{\text{screw}} = 0.5185 \text{ nm}$  and  $b_{\text{edge}} = 0.3189 \text{ nm}$ ). The values of screw dislocation density as calculated by using Eq. (1) are found to be  $5.03 \times 10^8$ ,  $9.17 \times 10^8$ , and  $1.45 \times 10^9 \text{ cm}^{-2}$ , whereas, the values of edge dislocation density are  $1.08 \times 10^{10}$ ,  $1.39 \times 10^{10}$ , and  $1.59 \times 10^{10} \text{ cm}^{-2}$  for GaN films with N/Ga ratios of 18.8, 29.4, and 40.1, respectively. In essence, the sample grown with N/Ga flux ratio of 18.8 has less dislocation density as compared to the samples with N/Ga flux ratios of 29.4 and 40.1.

Figure 3 shows the top view of SEM images of the GaN films grown with different N/Ga flux ratio. It was found that the GaN films exhibit pits on the surface. The average pit densities, as measured by SEM, were found to be  $1.18 \times 10^9$ ,  $1.48 \times 10^9$ , and  $1.97 \times 10^9 \text{ cm}^{-2}$  for samples with N/Ga ratios of 18.8, 29.4, and 40.1, respectively. The pit density increases with increasing N/Ga flux ratio. Such behavior could be due to the Ga-adlayer coverage.<sup>17-19</sup> The Ga-adlayer coverage decreases with increasing N/Ga ratio because of decreasing Ga adatom surface diffusion and results in the formation of pits on the GaN surface. The

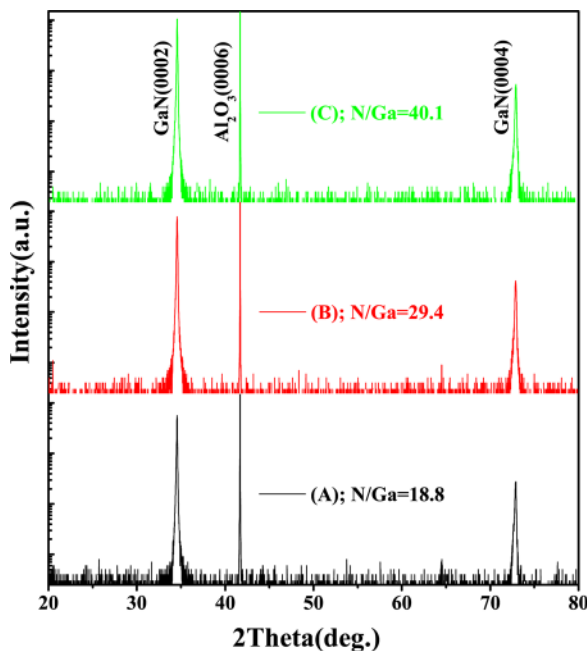


FIG. 1. (Color online)  $2\theta$ - $\omega$  HRXRD scanning curve of GaN films grown on sapphire substrate.

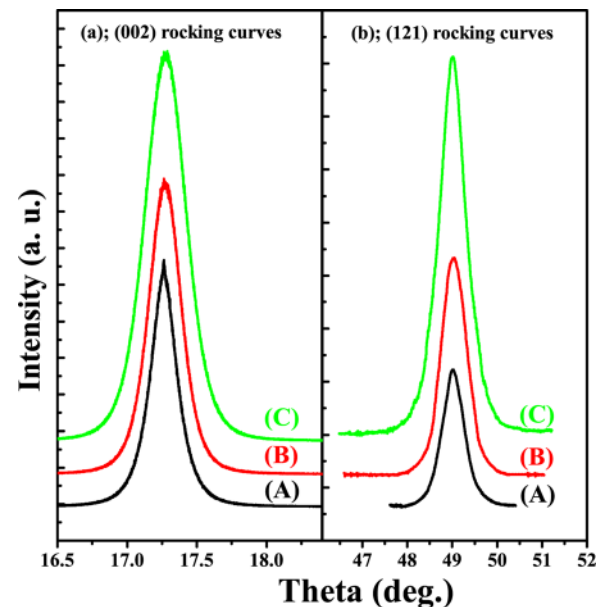


FIG. 2. (Color online) The XRC of the (002) and (121) GaN reflections.

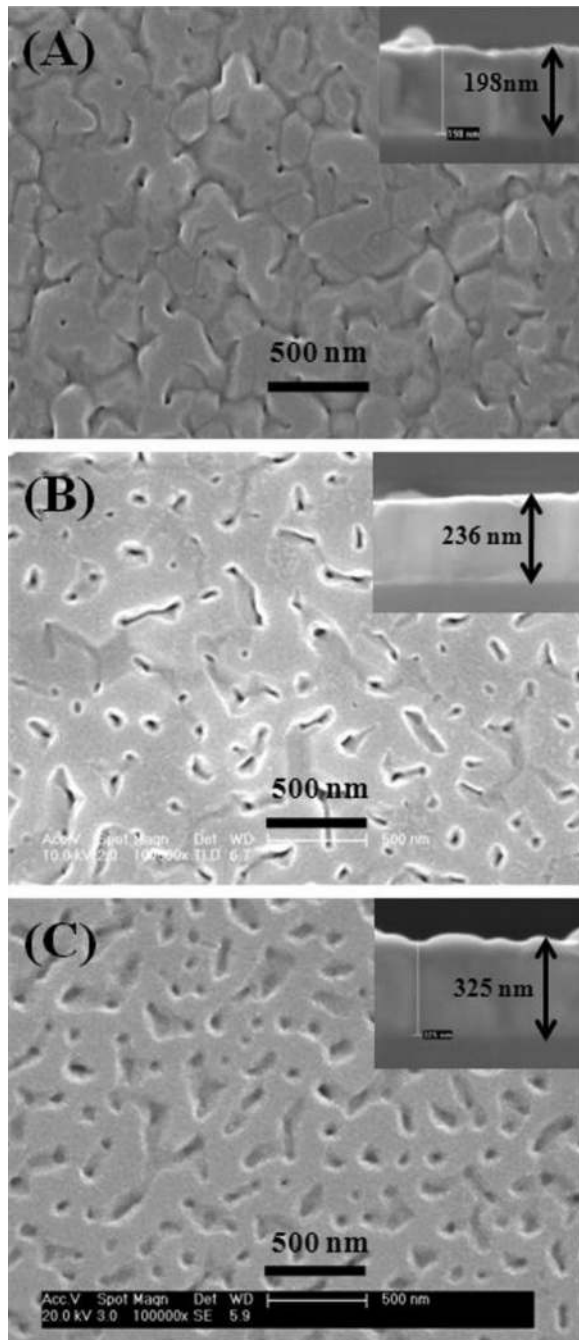


FIG. 3. FE-SEM images of GaN sample grown on sapphire substrate with N/Ga ratios of (a) 18.8, (b) 29.4, and (c) 40.1. The inset shows the cross-sectional SEM.

cross-sectional SEM images of the GaN films are shown in inset of Fig. 3. The thicknesses of the GaN films are 198, 236, and 325 nm with N/Ga ratios of 18.8, 29.4, and 40.1, respectively, as found from the cross-sectional SEM.

The room temperature PL spectrum of GaN grown with different N/Ga flux ratio is shown in Fig. 4(a). The spectrum exhibits an emission peak at around  $\sim 3.4$  eV, which is usually attributed to the free excitonic transition with radiative emission between valence and conduction bands of GaN. The normalized PL spectrum of GaN is shown in the inset of Fig. 4(a). The FWHM of the emission peak, which is used to reveal the crystal quality of the film, increases with increas-

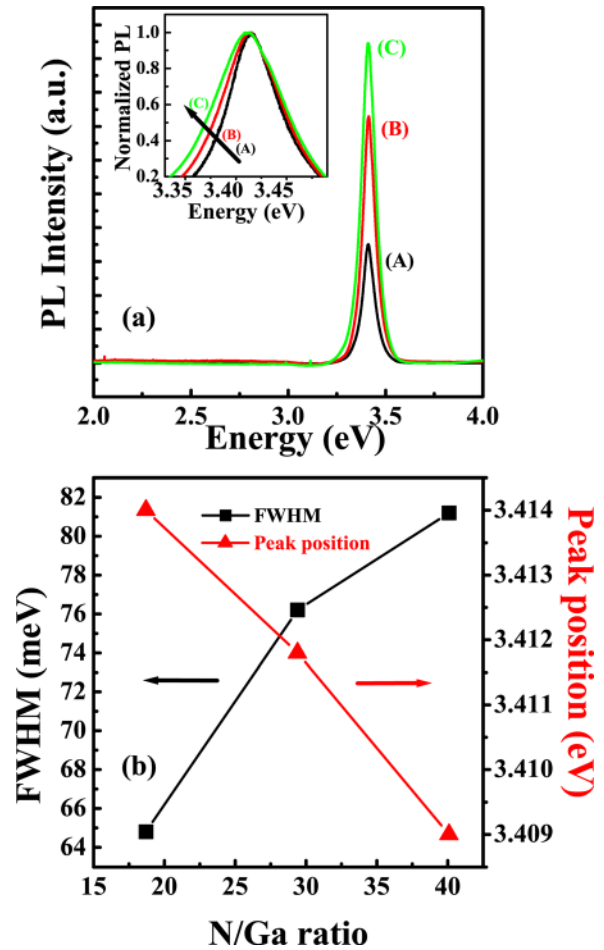


FIG. 4. (Color online) (a) The room-temperature photoluminescence spectra of GaN films grown on sapphire substrate. The inset shows the normalized PL spectra. (b) Variation of FWHM and peak position of PL spectra with N/Ga ratio.

ing N/Ga ratio. The variation of FWHM with flux ratio is given in Fig. 4(b). We also observed a slight shift in peak position with N/Ga ratio, i.e., the PL peak position observed at 3.414, 3.411, and 3.409 eV in GaN films with N/Ga ratios of 18.8, 29.4, and 40.1, respectively. It is known that the PL peak position shifts to a lower energy as the compressive stress in GaN films decreases.<sup>20</sup> The decrease in compressive stress with N/Ga ratio can also be attributed to the increase in film thickness.

In order to investigate and cross check the existence of strain, we have studied the room temperature Raman spectra and the results are shown in Fig. 5. Raman spectra displays  $E_2$  (high) phonon peaks of the GaN films along with substrate peaks assigned by an asterisk (\*). The  $E_2$  phonon mode in the spectra can be used to measure the strain of the films.<sup>21</sup>  $E_2$  mode is sensitive to the strain of the GaN crystal and the frequency value of the  $E_2$  mode of strain free GaN is  $568\text{ cm}^{-1}$ .<sup>22,23</sup> An enlarged view of the  $E_2$  peak is shown in the inset of Fig. 5. The  $E_2$  peak positions observed at 570.0, 569.4, and  $568.9\text{ cm}^{-1}$  in GaN films with N/Ga ratios of 18.8, 29.4, and 40.1, respectively, indicate that films are compressively stressed.<sup>24</sup> The amount of compressive strain decreases with increasing N/Ga ratio. It is observed from Fig. 5 that there is a shift in the  $E_2$  peak of the GaN films



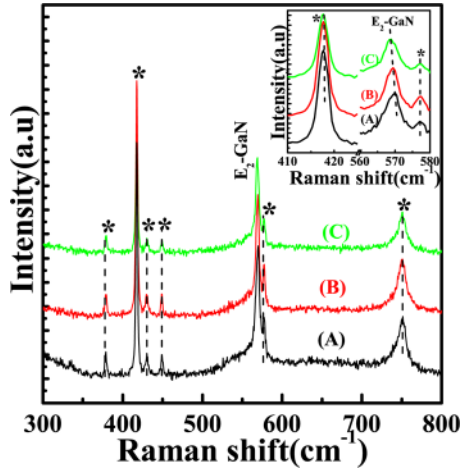


FIG. 5. (Color online) The room-temperature Raman spectra of GaN films grown on sapphire substrate with N/Ga ratios of (a) 18.8, (b) 29.4 and (c) 40.1. The inset shows the zoomed view of the  $E_2$  peak of GaN film along with substrate peaks.

with respect to the N/Ga ratio and is because of the different film thicknesses. The quantitative values of the compressive stress were obtained by using the relation<sup>25</sup>

$$\sigma = \Delta\omega/6.2 \text{ cm}^{-1}\text{GPa}^{-1}, \quad (2)$$

where  $\sigma$  is the biaxial compressive stress expressed in gigapascal, and  $\Delta\omega$  is the Raman shift in  $\text{cm}^{-1}$ . The values of  $\sigma$  were obtained as  $-0.322$ ,  $-0.237$ , and  $-0.151 \text{ cm}^{-1} \text{ GPa}^{-1}$  in GaN films with N/Ga ratios of 18.8, 29.4, and 40.1, respectively. Thus Raman spectra suggests the presence of strain in the films with respect to the different N/Ga ratio and is identical with the results obtained from room temperature PL measurements.

Figure 6 shows the room temperature  $I$ - $V$  characteristics of three Schottky diodes fabricated from GaN films with different N/Ga flux ratio. The schematic diagram of the diode is shown in the inset of Fig. 6. It was found that the rectifying

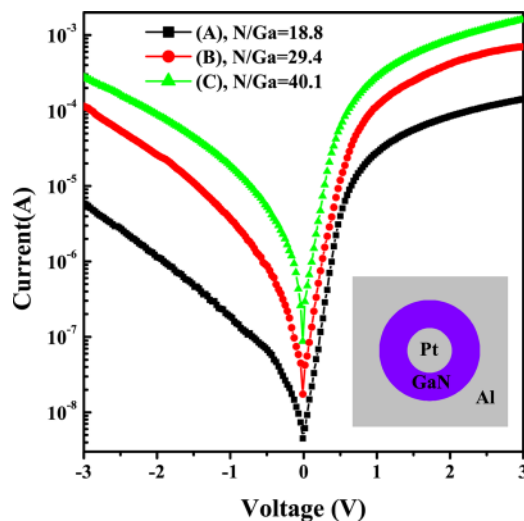


FIG. 6. (Color online) The room-temperature  $I$ - $V$  characteristics of Schottky diodes fabricated from GaN films grown on sapphire substrate with N/Ga ratios of (a) 18.8, (b) 29.4, and (c) 40.1. The inset shows the schematic diagram of the Schottky diode.

behavior of the diodes as defined as  $I_F/I_R(\text{on/off})$  at certain applied voltage is strongly dependent on the N/Ga ratio. The on/off ratios at 2 V are 74.39, 16.04, and 9.87 for the diodes with N/Ga ratios of 18.8, 29.4, and 40.1, respectively; i.e., the diode with N/Ga = 18.8 (sample (A)) has good rectifying nature and the rectifying nature of the diodes decreases with increasing N/Ga ratio. In addition, the leakage current at certain reverse bias increases with increasing N/Ga ratio. The leakage current at  $-2 \text{ V}$  is  $1.14 \times 10^{-6}$ ,  $2.62 \times 10^{-5}$ , and  $8.95 \times 10^{-5} \text{ A}$  for the diodes with N/Ga ratios of 18.8, 29.4, and 40.1, respectively. The increase in leakage current with N/Ga ratio may be due to an increase in pit density as well as screw dislocation density.<sup>26,27</sup> The dislocations in the GaN films act as localized conducting paths, resulting in the increase in leakage current and hence a decrease in the device performance.

In order to determine the current transport mechanism present in the Schottky diodes, we have performed room temperature Hall measurements to get the carrier concentration in the GaN films. The existence of a certain transport mechanism in a metal/semiconductor interface can be predicted by the ratio between the characteristic energy ( $E_{00}$ ) and the thermal energy  $kT$ . The characteristic energy ( $E_{00}$ ) is a parameter related to the tunneling transmission probability that the electron tunnel the barrier and is given by<sup>28</sup>

$$E_{00} = \frac{h}{4\pi} \left( \frac{N_D}{m^* \epsilon_s} \right)^{1/2}, \quad (3)$$

where  $N_D$  is the carrier concentration of GaN films,  $m^*$  is the effective mass of the electron, and  $\epsilon_s$  is the dielectric constant of GaN. In particular, thermionic emission (TE) is effective whenever  $E_{00}/kT \ll 1$ . On the other hand, thermionic field emission (TFE) is predominant when  $E_{00}/kT \approx 1$ , while the field emission (FE) transport dominates when  $E_{00}/kT \gg 1$ .<sup>29</sup> The carrier concentration as found from the room temperature Hall measurements are  $1.7 \times 10^{17}$ ,  $4.2 \times 10^{17}$ , and  $6.4 \times 10^{17} \text{ cm}^{-3}$  in the GaN films with N/Ga ratios of 18.8, 29.4, and 40.1, respectively. Taking the values of  $m^* = 0.2m_0$  and  $\epsilon_s = 9.5\epsilon_0$ , the value of  $E_{00}/kT$  at room temperature was found to be 0.21, 0.33, and 0.41 for the diodes with N/Ga ratios of 18.8, 29.4, and 40.1, respectively. Since  $E_{00}/kT \ll 1$ , the current transport in the present case is dominated by TE. According to TE theory, where  $qV > 3kT$ , the forward  $I$ - $V$  characteristic of a Schottky diode is given by<sup>30-32</sup>

$$I = I_s \exp \left[ \frac{q(V - IR_s)}{\eta kT} \right], \quad (4)$$

$$\text{with } I_s = AA^* T^2 \exp \left( -\frac{\phi_b}{kT} \right), \quad (5)$$

where  $I_s$  is the saturation current density,  $T$  is the absolute temperature,  $A$  is the active device area,  $A^*$  is the Richardson's constant,  $k$  is the Boltzmann constant,  $q$  is the electron charge,  $\phi_b$  is the Schottky barrier height, and  $\eta$  is the ideality factor. The values of  $\phi_b$  and  $\eta$  for the Schottky diodes were calculated by fitting Eq. (4) in the linear region of the forward  $I$ - $V$  curves ignoring the series resistance ( $R_s$ ), as shown

in Fig. 7. The value of  $A^*$  for GaN was taken as  $26.4 \text{ Acm}^{-2}\text{K}^{-2}$ .<sup>33</sup> for our calculations. The values of barrier height ( $\phi_b$ ) were found to be 0.73, 0.67, and 0.62 eV, while the values of ideality factor ( $\eta$ ) found to be 2.5, 2.9, and 3 for the diodes with N/Ga ratios of 18.8, 29.4, and 40.1, respectively. The higher value of barrier height (0.73 eV) and lower value of ideality factor (2.5) of the diode fabricated from GaN film with N/Ga = 18.8 indicates a good rectifying nature among them. From Fig. 7, it is seen that only a small region of the  $I$ - $V$  curve is linear, while most of the curve is nonlinear. At higher voltages, the current seems to saturate and generally the series resistance appears to dominate the conduction process in this region. Fitting of Eq. (4) without neglecting series resistance did not follow the measured  $I$ - $V$  characteristics of three diodes. This result illustrates that in the present case, the thermionic emission over the Schottky barrier is suppressed at higher applied voltages by other current transport mechanisms. At higher applied volt-

age, the current transport follows power-law ( $I \sim V^{1.6}$ ). This power law is generally attributed to the space-charge-limited current (SCLC) mechanism,<sup>34</sup> which is observed in the wide bandgap semiconductors. The SCLC mechanism is due to the presence of trapping centers in the GaN films. In undoped GaN films, different kinds of trap levels are present, like nitrogen vacancies, point defects along the dislocation sites and dislocation induced defects,<sup>35</sup> which act as non-radiative recombination sites and hence controlling the current transport mechanisms at higher applied voltage. In SCLC region, the current conduction strongly depends on the concentration as well as the energy distribution of trapping centers present inside the GaN films. The concentration of trapping centers ( $N_t$ ) was found out approximately by using the following relation:<sup>36</sup>

$$V_1 \simeq \frac{qN_t L^2}{\epsilon_s}, \quad (6)$$

where  $V_1$  is the onset of SCLC conduction process,  $L$  is the thickness of the GaN epilayers,  $q$  is the electron charge, and  $\epsilon_s$  is the dielectric permittivity of the semiconductor. The onsets of SCLC are 0.56, 0.53, and 0.47 V for the diodes with N/Ga ratios of 18.8, 29.4, and 40.1, respectively. Considering the proper values of  $V_1$ ,  $\epsilon_s$ , and  $L$ , the values of  $N_t$  were found to be  $7.5 \times 10^{15}$ ,  $5.0 \times 10^{15}$ , and  $2.33 \times 10^{15} \text{ cm}^{-3}$  the diodes with N/Ga ratios of 18.8, 29.4, and 40.1, respectively.

#### IV. CONCLUSION

Effects of N/Ga flux ratio on structural, morphological, and optical properties of GaN films and on electrical transport properties of Pt/GaN Schottky diodes have been studied. The N/Ga flux ratio is found to play a major role in controlling crystal quality, morphology, and emission properties of GaN films and also on electrical transport property of Pt/GaN Schottky diodes. The room temperature photoluminescence study reveals a shift in the band-edge emission toward the lower energy with an increase in N/Ga ratio and is attributed to the decrease in compressive stress in the films. The electrical transport properties of Pt/GaN Schottky diodes show a significant increase in leakage current with increase in N/Ga ratio, and it is due to the increase in pit density as well as an increase in dislocation density on the GaN films.

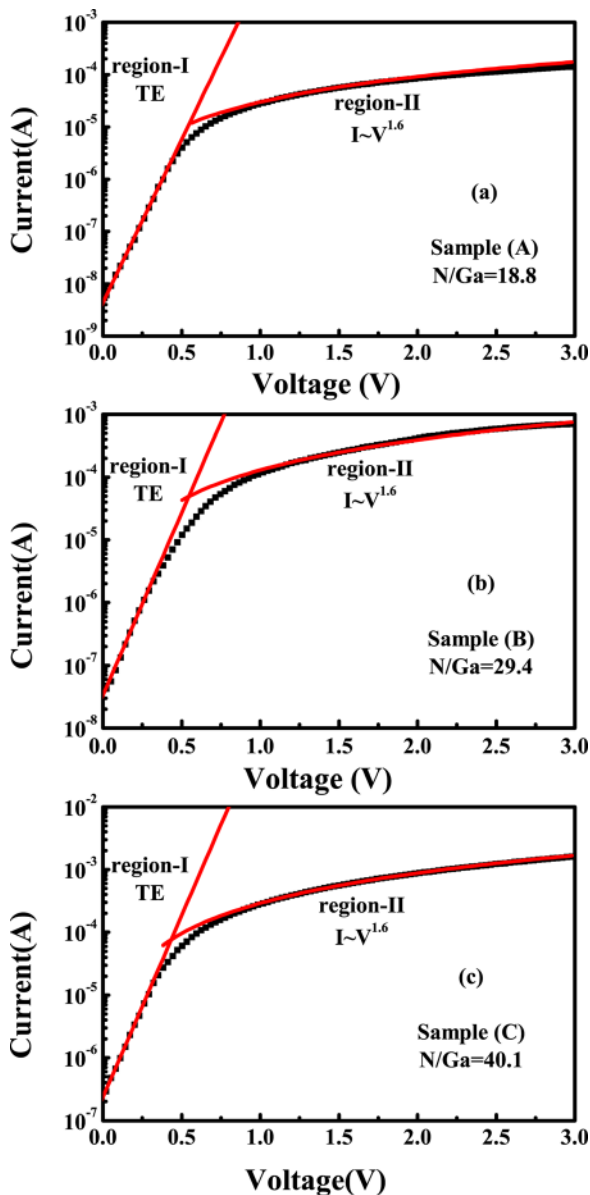


FIG. 7. (Color online) (a)–(c) Semi-log plots of  $I$ - $V$  characteristics under forward bias.

<sup>1</sup>S. Nakamura, M. Senoh, N. Iwasa, and S. Nagahama, *Appl. Phys. Lett.* **67**, 1868 (1995).

<sup>2</sup>M. A. Kahn, A. Bhattarai, J. N. Kuzina, and D. T. Olsen, *Appl. Phys. Lett.* **63**, 1214 (1993).

<sup>3</sup>H. Morkoç, S. Strite, G. B. Gao, M. E. Lin, B. Sverdlov, and M. Burns, *J. Appl. Phys.* **76**, 1363 (1994).

<sup>4</sup>E. Munoz, E. Monroy, J. L. Pau, F. Calle, F. Omnès, and P. Gibart, *J. Phys.: Condens. Matter* **13**, 7115 (2001).

<sup>5</sup>M. Asif Khan, M. S. Shur, J. N. Kuznia, Q. Chen, J. Burm, and W. Schaff, *Appl. Phys. Lett.* **66**, 1083 (1995).

<sup>6</sup>J. F. Muth, J. H. Lee, I. K. Shmagin, R. M. Kolbas, H. C. Casey, B. P. Keller, U. K. Mishra, and S. P. DenBaars, *Appl. Phys. Lett.* **71**, 2572 (1997).

<sup>7</sup>R. Averbeck and H. Riechert, *Phys. Status Solidi A* **176**, 301 (1999).

<sup>8</sup>T. Böttcher, S. Einfeldt, V. Kirchner, S. Figge, H. Heinke, D. Hommel, H. Selke, and P. L. Ryder, *Appl. Phys. Lett.* **73**, 3232 (1998).

<sup>9</sup>C. Adelman, R. Langer, G. Feuillet, and B. Daudin, *Appl. Phys. Lett.* **75**, 3518 (1999).

- <sup>10</sup>R. C. Powell, N. E. Lee, Y. W. Kim, and J. E. Greene, *J. Appl. Phys.* **73**, 189 (1993).
- <sup>11</sup>W. Qian, M. Skowronski, M. D. Graef, K. Doverspike, L. B. Rowland, and D. K. Gaskill, *Appl. Phys. Lett.* **66**, 1544 (1995).
- <sup>12</sup>V. Narayanan, K. Lorenz, W. Kim, and S. Mahajan, *Appl. Phys. Lett.* **78**, 1544 (2001).
- <sup>13</sup>Z. Yu, M. A. L. Johnson, J. D. Brown, N. A. El-Masry, J. W. Cook, and J. F. Schetzina, *J. Cryst. Growth* **195**, 333 (1998).
- <sup>14</sup>X. Q. Shen, H. Matsuhata, and H. Okumura, *Appl. Phys. Lett.* **86**, 021912 (2005).
- <sup>15</sup>B. Heying, X. H. We, S. Keller, Y. Li, D. Kapolnek, B. P. Keller, S. P. Denbaars, and J. S. Speck, *Appl. Phys. Lett.* **68**, 643 (1996).
- <sup>16</sup>T. Metzger, R. Höpler, E. Born, O. Ambacher, M. Stutzmann, R. Stömmer, M. Schuster, H. Göbel, S. Christiansen, M. Albrecht, and H. P. Strunk, *Philos. Mag. A* **77**, 1013 (1998).
- <sup>17</sup>B. Heying, R. Averbeck, L. F. Chen, E. Haus, H. Riechert, and J. S. Speck, *J. Appl. Phys.* **88**, 1855 (2000).
- <sup>18</sup>E. J. Tarsa, B. Heying, X. H. Wu, P. Fini, S. P. DenBaars, and J. S. Speck, *J. Appl. Phys.* **82**, 5472 (1997).
- <sup>19</sup>A. Hierro, A. R. Arehart, B. Heying, M. Hansen, U. K. Mishra, S. P. DenBaars, J. S. Speck, and S. A. Ringel, *Appl. Phys. Lett.* **80**, 805 (2002).
- <sup>20</sup>W. Rieger, T. Metzger, H. Angerer, R. Dimitrov, O. Ambacher, and M. Stutzmann, *Appl. Phys. Lett.* **68**, 970 (1996).
- <sup>21</sup>F. Demangeot, J. Frandon, M. A. Renucci, O. Briot, B. Gil, and R. L. Aulombard, *Solid State Commun.* **100**, 207 (1996).
- <sup>22</sup>V. Lemos, C.A. Arguello, and R. C. C. Leite, *Solid State Commun.* **11**, 1351 (1972).
- <sup>23</sup>A. Cingolani, M. Ferrara, M. Lugarà, and G. Scamarcio, *Solid State Commun.* **58**, 823 (1986).
- <sup>24</sup>J. F. Wang, D. Z. Yao, J. Chen, J. J. Zhu, D. G. Zhao, D. S. Jiang, and J. W. Liang, *Appl. Phys. Lett.* **89**, 152105 (2006).
- <sup>25</sup>T. Kozawa, T. Kachi, H. Kano, H. Nagase, N. Koide, and K. Manabe, *J. Appl. Phys.* **77**, 4389 (1995).
- <sup>26</sup>E. J. Miller, D. M. Schaadt, E. T. Yu, X. L. Sun, L. J. Brillson, P. Waltereit, and J. S. Speck, *J. Appl. Phys.* **94**, 7611 (2003).
- <sup>27</sup>J. Miller, E.T. Yu, P. Waltereit, and J. S. Speck, *Appl. Phys. Lett.* **84**, 535 (2004).
- <sup>28</sup>K. Cinar, N. Yildirim, C. Coskun, and A. Turut, *J. Appl. Phys.* **106**, 073717 (2009).
- <sup>29</sup>R. T. Tung, *Mater. Sci. Eng. R* **35**, 1 (2001).
- <sup>30</sup>B. Roul, M. K. Rajpalke, T. N. Bhat, M. Kumar, N. Sinha, A. T. Kalgatgi, and S. B. Krupanidhi, *J. Appl. Phys.* **109**, 044502 (2011).
- <sup>31</sup>H. Morkoç, *Handbook of Nitride Semiconductors and Devices* (Wiley-VCH, Berlin, 2008).
- <sup>32</sup>M. Shur, *Physics of Semiconductor Devices* (Prentice-Hall, Engelwood Cliffs, 1990).
- <sup>33</sup>M. Sawada, T. Sawada, Y. Yanagata, K. Imai, H. Kimura, M. Yoshino, K. Iizuka, and H. Tomozawa, *J. Cryst. Growth* **189-190**, 706 (1998).
- <sup>34</sup>X. M. Shen, D. G. Zhao, Z. S. Liu, Z. F. Hu, H. Yang, and J. W. Liang, *Solid-State Electron.* **49**, 847 (2005).
- <sup>35</sup>C. B. Soh, S. J. Chua, H. F. Lim, D. Z. Chi, S. Tripathy, and W. Liu, *J. Appl. Phys.* **96**, 1341 (2004).
- <sup>36</sup>M. A. Lampert and P. Mark, *Current Injection in Solids* (Academic, New York, 1970).